Hyperspherical partial wave theory with two-term error correction

S. Paul*

Theory Group, Physical Research Laboratory, Navrangpura, Ahmedabad 380 009, India

(Received 1 February 2008; published 28 May 2008)

Hyperspherical partial wave theory has been applied to calculate *T*-matrix elements and single differential cross-section (SDCS) results for electron-hydrogen ionization processes within the Temkin-Poet model potential. We considered three different values of step length to compute the radial part of final state wave function. Numerical outcomes show that *T*-matrix elements and SDCS values depend on the step length *h*. Here, we have presented *T*-matrix elements and the corresponding SDCS results for 0.0075, 0.009, and 0.01 a.u. values of *h* and for 27.2, 40.8, and 54.4 eV impact energies. With the help of the calculated data for three different step lengths, we have been able to evaluate a two-term error function depending on the step length *h*. Finally, two-term error corrected *T*-matrix elements and the corresponding SDCS values have been computed. We fitted our two-term error corrected SDCS results by a suitable curve and compared with the benchmark results of Jones *et al.* [Phys. Rev. A **66**, 032717 (2002)]. Our fitted curves agree very well with the calculated results of Jones *et al.* and two-term error corrected SDCS results show fair agreement with the benchmark results. Two-term error corrected SDCS results are significantly better than the calculated SDCS results of different step lengths.

DOI: 10.1103/PhysRevA.77.052714 PACS number(s): 34.80.Dp, 34.10.+x, 34.50.Fa

I. INTRODUCTION

The electron-impact ionization of hydrogen probes the correlated quantal dynamics of two electrons moving in the long-range Coulomb field of a third body. As such it remains one of the most fundamental and interesting problems in nonrelativistic quantum mechanics. There are many attempts for a complete solution but all of these face enormous difficulties and have only limited success. Among these the most successful attempts are the method of convergent close-coupling (CCC) and exterior complex scaling (ECS). Another promising approach for the electron-hydrogen atom ionization problem is the hyperspherical partial wave (HPW) approach. After the successful applications of HPW theory to compute triple differential equal-energy-sharing cross-section results [1–6], we aspire to calculate single differential cross-section (SDCS) results. Before considering the full electron-hydrogen ionization problem, here, we consider a Coulomb three-body system within the Temkin-Poet (TP) model [7,8]. The TP model of electron-hydrogen collision is now widely considered to be an ideal testing ground for the improvement of general methods intended for the full Coulomb three-body problem. In this context, the calculated SDCS results of other theories for the TP model potential are praiseworthy. Among these, the attempt of Jones *et al.* [9,10] is remarkable as they obtained benchmark results. They developed a variable-spacing finite-difference algorithm that rapidly propagates the general solution of the Schrödinger equation to large distances, originally used by Poet [11] to solve the TP model. The ECS calculation is generally in good agreement with the benchmark results of Jones *et al.* except at the extreme asymmetric energy sharing [13]. The calculated singlet SDCS curves of CCC method are wavy, Bray considered a smooth curve by educated guess [12]. The CCC results agree nicely with benchmark results of Jones *et al.* only for the triplet case (generally, CCC does not yield convergent amplitude for the triplet case, except for total angular momentum zero). We also note the work of Miyashita *et al.* [14]. They have presented SDCSs for total energies of 4, 2, and 0.1 Ry using two different methods. One produces an asymmetric energy distribution similar to that of CCC while the other gives a symmetric distribution. Both contain oscillations. It should be noted that recently, we have used the HPW approach to calculate SDCS results for the full electron-hydrogen-ionization problem at 60 eV incident energy [15]. The resultant curve was wavy and calculated cross-section results are irrelevant at extreme energy sharing. We fitted our calculated SDCS data by a fourth order parabola and compared with the experimental values of Shyn [16]. Our fitted curve agrees with the experimental results excellently. In this article we present the SDCS results for the TP model using the HPW method with two-term error correction. Here, we introduce a procedure to calculate the error function. The results are obtained for intermediate (27.2, 40.8, and 54.4 eV) energies. We have calculated *T*-matrix elements and the corresponding SDCS data for three different values of step length *h* (0.0075, 0.009, and 0.01 a.u.), used to calculate the radial part of final state wave function numerically. Numerical observation shows that the *T*-matrix elements depend on *h*. Using the data of various step lengths, we calculated a two-term error function depending on *h*. Finally, two-term error corrected SDCS values were computed. The nature of error corrected SDCS undulating curves suggest a fit with a proper function. The HPW method for the TP model is reproduced in Sec. II, procedure of calculation is presented in Sec. III, two-term error correction process is given in Sec. IV, results are presented in Sec. V with a short discussion, and some concluding remarks are found in Sec. VI. Atomic units are used throughout this paper except where otherwise noted.

*spaul@pub.iams.sinica.edu.tw

II. THEORY

The T-matrix element, we use in cross-section calculation, is given by

$$T_{fi}^{s} = \langle \Psi_{fs}^{(-)} | V_i | \Phi_i \rangle. \tag{1}$$

In this expression Φ_i is the unperturbed initial channel wave function, satisfying certain exact boundary condition at large distance and V_i is the corresponding perturbation potential. Here, $\Psi_{fs}^{(-)}$ is the symmetrized scattering state (see Ref. [17] for a definition). For information regarding electron-hydrogen ionization within the TP model potential, one may solve the corresponding Schrödinger equation. We start by writing the Schrödinger equation for the full electron-hydrogen ionization problem

$$\left[-\frac{1}{2}\nabla_{\vec{r}_1}^2 - \frac{1}{2}\nabla_{\vec{r}_2}^2 - \frac{1}{r_1} - \frac{1}{r_2} + V_{12} \right] \Psi_{fs}^{(-)} = E \Psi_{fs}^{(-)}, \tag{2}$$

where

$$V_{12} = \frac{1}{|\vec{r}_1 - \vec{r}_2|}. \tag{3}$$

To calculate the final channel symmetrized continuum state $\Psi_{fs}^{(-)}$ we use hyperspherical coordinate $R=\sqrt{r_1^2+r_2^2}$, $\alpha = \arctan(r_2/r_1)$, $\hat{r}_1=(\theta_1,\phi_1)$, $\hat{r}_2=(\theta_2,\phi_2)$, and $\omega=(\alpha,\hat{r}_1,\hat{r}_2)$. Also we set $P=\sqrt{p_1^2+p_2^2}$, $\alpha_0=\arctan(p_2/p_1)$, $\hat{p}_1=(\theta_{p_1},\phi_{p_1})$, $\hat{p}_2=(\theta_{p_2},\phi_{p_2})$, and $\omega_0=(\alpha_0,\hat{p}_1,\hat{p}_2)$, where $\vec{r}_i$ and $\vec{p}_i$ $(i=1,2)$ are the coordinates and momenta of ith charged particles. $\Psi_{fs}^{(-)}$ is then expanded in symmetrized hyperspherical harmonics [1] that are functions of five angular variables and l_1,l_2,n,L,M, which are, respectively, the angular momenta of two electrons, the order of the Jacobi polynomial in hyperspherical harmonics, the total angular momentum, and its projection. For a given symmetry s ($s=0$ for singlet and $s=1$ for triplet), we decompose the final state as

$$\Psi_{fs}^{(-)} = \sqrt{\frac{2}{\pi}} \sum_{\mu} \frac{F_{\mu}^{s}(\rho)}{\rho^{5/2}} \phi_{\mu}^{s}(\omega) \tag{4}$$

where μ is the composite index (l_1,l_2,n,L,M) and $\rho=PR$ and $\phi_{\mu}^{s}(\omega)$ are orthogonal functions that are product of Jacobi polynomial $P_{l_1 l_2}^{n}$ and coupled angular momentum eigenfunction $Y_{l_1 l_2}^{LM}(\hat{r}_1,\hat{r}_2)$ [1]. $F_{\mu}^{s}(\rho)$ then satisfy the infinite coupled differential equations

$$\left[\frac{d^2}{d\rho^2} + 1 - \frac{\nu_\lambda(\nu_\lambda+1)}{\rho^2} \right] F_{\mu}^{s}(\rho) + \sum_{\mu'} \frac{2\alpha_{\mu\mu'}^{s}}{\rho} F_{\mu'}^{s}(\rho) = 0. \tag{5}$$

Here $\alpha_{\mu\mu'}^{s}$ are the matrix elements of the full three-body interaction potential and $\nu_\lambda=\lambda+3/2$ where $\lambda=2n+l_1+l_2$.

For the cusp model (or TP model) the V_{12} term, derived from the first term of the partial-wave expansion of the electron-electron potential, is given by

$$V_{12} = \frac{1}{r_>} = \frac{1}{\max(r_1,r_2)}. \tag{6}$$

The TP model calculated in this article is simplification of our earlier calculated full electron-hydrogen problem, and we only consider the case where all angular momenta are zero. Retaining only zero angular momentum terms we have

$$\Psi_{fs}^{(-)} = \sqrt{\frac{2}{\pi}} \sum_{n} \frac{F_{n}^{s}(\rho)}{\rho^{5/2}} \phi_{n}^{s}(\omega), \tag{7}$$

where $\phi_n^s = \phi_{(L=l_1=l_2=0),n}^{s}$. The expression of hyperspherical harmonics where all angular momenta are zero is given by

$$\phi_{(L=l_1=l_2=0),n}^{s}(\omega) = \frac{1}{2}\{1+(-1)^{s+n}\} P_{00}^{n}(\alpha) Y_{00}^{00}(r_1,r_2). \tag{8}$$

The radial functions $F_n^s(\rho)$ satisfy an infinite coupled set of equations

$$\left[\frac{d^2}{d\rho^2} + 1 - \frac{\nu_n(\nu_n+1)}{\rho^2} \right] F_{n}^{s}(\rho) + \sum_{n'} \frac{2\alpha_{nn'}^{s}}{\rho} F_{n'}^{s}(\rho) = 0. \tag{9}$$

In the above expression

$$\alpha_{nn'}^{s} = -\langle \phi_n^s | C | \phi_{n'}^s \rangle / P \tag{10}$$

and

$$C = -\frac{1}{\cos\alpha} - \frac{1}{\sin\alpha} + \frac{1}{\max(\cos\alpha,\sin\alpha)}. \tag{11}$$

Finally, one obtains the T-matrix element in the form [for details see Eq. (25) of Ref [1]]:

$$T_{fi}^{s} = \sum_{n} C^{s}(n) \phi_{n}^{s}(\omega_0). \tag{12}$$

The modulus square of the T-matrix element, which is used to calculate differential cross section, is then given by

$$|T_{fi}^{s}|^2 = \sum_{nn'} T_{nn'}^{s} \phi_{n}^{s}(\omega_0) \phi_{n'}^{s*}(\omega_0). \tag{13}$$

III. PRESENT CALCULATION

In our present calculation n, the degree of the Jacobi polynomial, was varied from 0 to 11. We considered $n=0$, 2, 4, 6, 8, 10 for calculating singlet SDCS results and $n=1$, 3, 5, 7, 9, 11 for computing triplet SDCS values [18]. The main numerical task is to calculate the radial functions $F_n^s(\rho)$ over a wide domain $[0,\infty)$. As in Ref. [1], we divide the whole solution interval $[0,\infty)$ into three subintervals $[0,\Delta]$, $(\Delta,R_0]$, and $[R_0,\infty)$, where Δ has the value of a few atomic unit and R_0 is the asymptotic matching parameter. R_0 is needed to be such that $R_0 \sim 1/\sqrt{E}$, where E is the energy in the final channel [1]. Thus for energies of 27.2, 40.8, and 54.4 eV this range parameter R_0 may be chosen greater than the values 5000, 3000, and 2500 a.u., respectively. We have chosen R_0 around these values in our calculations. For $[R_0,\infty)$ we have the simply analytic solution [1]. We applied a seven-point

finite difference scheme [3] for solution in the initial interval $[0,\Delta]$ with step length h. Implementation of the ECS method involves solving very large and sparse system of linear equations, making its application to a four-body problem impractical with current supercomputing technology. In CCC calculations, it is necessary to solve the linear system of the form $AX=B$, where A is a real symmetric matrix. The matrix A occupies a large storage space. The computational task of HPW approach is simpler than that of ECS and CCC methods. Now for the difference equations we divided the domain $[0,\Delta]$ into 100 subintervals of length h and $\Delta=100h$. Solution over (Δ,R_0) is very simple. Because of the simple structure of Eq. (9) a Taylor series expansion method with step length $2h$ works nicely. Presently, we considered three different values of step length h, these are 0.0075, 0.009, and 0.01 a.u., respectively. Finally, we calculated $T^s_{nn'}$ and SDCS results for three different step lengths.

IV. TWO-TERM ERROR CORRECTION

In the previous section, we reproduced the values of $T^s_{nn'}$ for three different step lengths and observed that $T^s_{nn'}$ are varied with h. Now, we can consider a relation between $T^s_{nn'}(h)$ with the error term $E^s_{nn'}(h)$ as

$$T^s_{nn'}(h) = T^{s*}_{nn'} + E^s_{nn'}(h), \tag{14}$$

where $T^{s*}_{nn'}$ are the converged results with respect to the step length h. Since in our seven-point finite difference scheme the error term is $Kh^8f^{(8)}(\xi)$ [3] where K is a constant and ξ is a linear function of h. The error term of $T^s_{nn'}(h)$ calculation is $Ch^8f^{(8)}(\xi)$ where C is a constant. The error term reduced, as well as h decries. But there is a certain limitation on the choice of step length h. For example, if we look at $h=0.001$, the number of mesh points for the interval $(\Delta,\ R_0]$ becomes $1000R_0$. For $R_0=3000$ a.u., it will be 3000000. It is quite difficult to manage such a large grid points and it will also take much time for a single run. Instead of $Kh^8f^{(8)}(\xi)$, we can write the error term of seven-point finite difference scheme as

$$K_1h^8f^{(8)}(R_m) + K_2h^{10}f^{(10)}(R_m) + K_3h^{12}f^{(12)}(\xi),$$

for a certain grid point R_m. Using the above expression, we can easily formulate

$$E^s_{nn'}(h) = A^s_{nn'}h^8 + B^s_{nn'}h^{10} + G^s_{nn'}h^{12}f^{(12)}(\xi), \tag{15}$$

where $A^s_{nn'}$, $B^s_{nn'}$, and $G^s_{nn'}$ are independent of h. Considering first two terms, we get the expression of two-term error function for $T^s_{nn'}(h)$ elements

$$E^{s(2)}_{nn'}(h) = A^s_{nn'}h^8 + B^s_{nn'}h^{10}. \tag{16}$$

Corresponding two-term error corrected $T^{s*(2)}_{nn'}(h)$ elements satisfy the equation

$$T^s_{nn'}(h) = T^{s*(2)}_{nn'} + E^{s(2)}_{nn'}(h). \tag{17}$$

In the present context, we have considered step lengths of three different values h_1, h_2, and h_3. Therefore, from the Eq. (17) we have

$$E^{s(2)}_{nn'}(h_i) - E^{s(2)}_{nn'}(h_j) = T^s_{nn'}(h_i) - T^s_{nn'}(h_j) \tag{18}$$

for $i,j=1,\ 2,\ 3$ and $i\neq j$. The coefficients of h^8 and h^{10} in the expression (16) are given by

$$A^s_{nn'} = \frac{(h_3^{10}-h_2^{10})\{T^s_{nn'}(h_2)-T^s_{nn'}(h_1)\} - (h_2^{10}-h_1^{10})\{T^s_{nn'}(h_3)-T^s_{nn'}(h_2)\}}{(h_2^8-h_1^8)(h_3^{10}-h_2^{10}) - (h_3^8-h_2^8)(h_2^{10}-h_1^{10})},$$

$$B^s_{nn'} = -\frac{(h_3^8-h_2^8)\{T^s_{nn'}(h_2)-T^s_{nn'}(h_1)\} - (h_2^8-h_1^8)\{T^s_{nn'}(h_3)-T^s_{nn'}(h_2)\}}{(h_2^8-h_1^8)(h_3^{10}-h_2^{10}) - (h_3^8-h_2^8)(h_2^{10}-h_1^{10})}. \tag{19}$$

Here we have considered $h_1=0.0075$, $h_2=0.009$, and $h_3=0.01$ so the above expression of $A^s_{nn'}$ and $B^s_{nn'}$ reduce to

$$A^s_{nn'} = 0.05229064077\{T^s_{nn'}(h_2)-T^s_{nn'}(h_1)\} - 0.023472188\{T^s_{nn'}(h_3)-T^s_{nn'}(h_2)\},$$

$$B^s_{nn'} = -0.01143107936\{T^s_{nn'}(h_2)-T^s_{nn'}(h_1)\} + 0.006630530581\{T^s_{nn'}(h_3)-T^s_{nn'}(h_2)\}. \tag{20}$$

After calculating the $T^{s*(2)}_{nn'}$ elements, we have calculated the corresponding two-term error corrected SDCS results.

V. RESULTS AND DISCUSSION

As we discussed in Sec. III, we have considered six different values of the degree of Jacobi polynomial. There are total 36 pairs of (n,n') in the calculation of $T^s_{nn'}$. We have labeled those pairs by an integer variable P, varied from 1 to 36. The values of $T^0_{nn'}$ (zero indicates singlet) for three different step lengths and $T^{0*(2)}_{nn'}$ are presented in Fig. 1 for 27.2

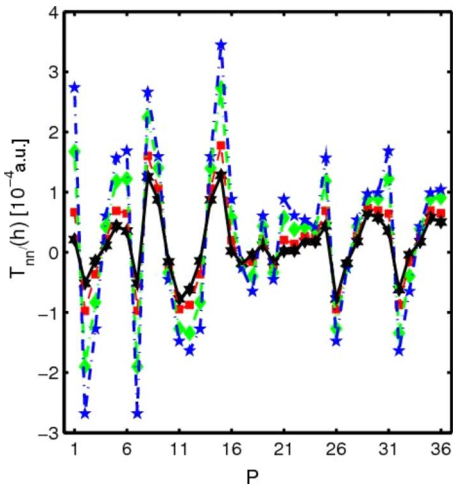

FIG. 1. (Color online) The values of $T^{0}_{nn'}$ (zero indicates singlet) for three different step lengths at 27.2 eV incident electron energy. Square points for $h=0.0075$, diamond points for $h=0.009$, and pentagon points for $h=0.01$. Hexagon points represent the values of $T^{0*(2)}_{nn'}$ at the same energy.

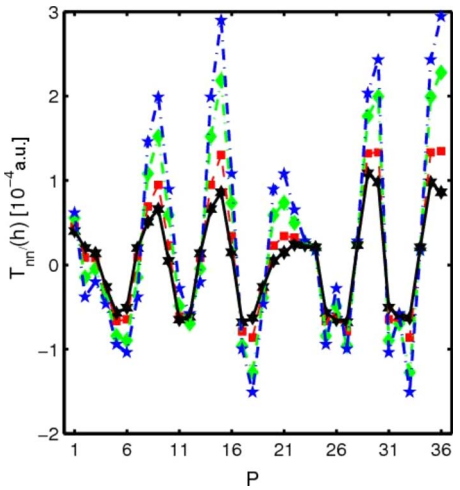

FIG. 2. (Color online) Same as in Fig. 1 but for the triplet case.

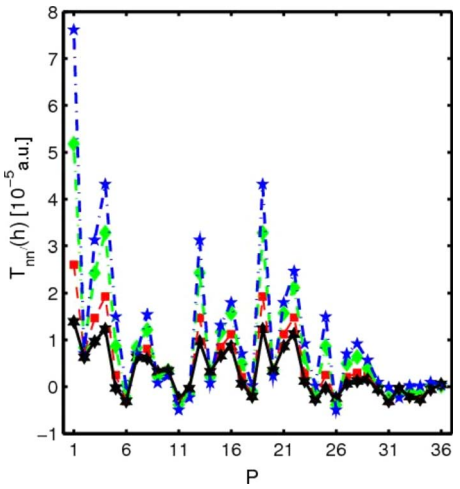

FIG. 3. (Color online) Same as in Fig. 1 but for 40.8 eV incident electron energy.

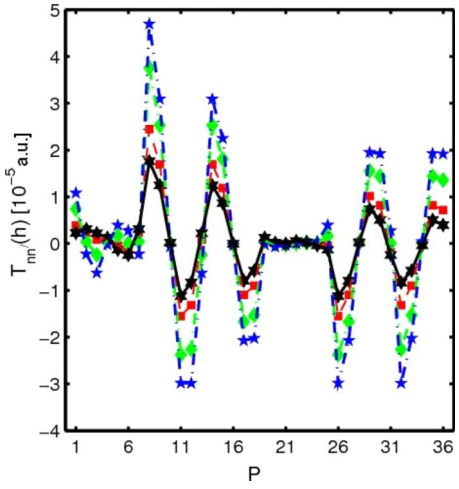

FIG. 4. (Color online) Same as in Fig. 3 but for the triplet case.

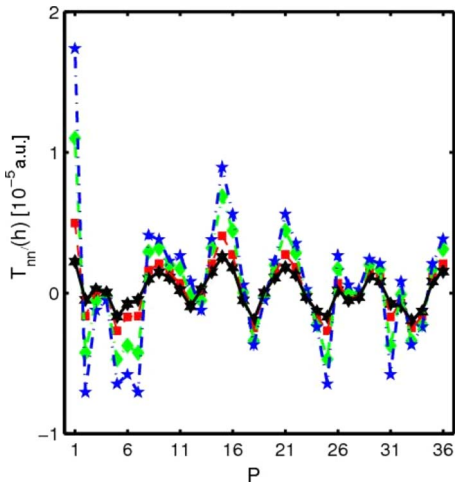

FIG. 5. (Color online) Same as in Fig. 1 but for the 54.4 eV incident electron energy.

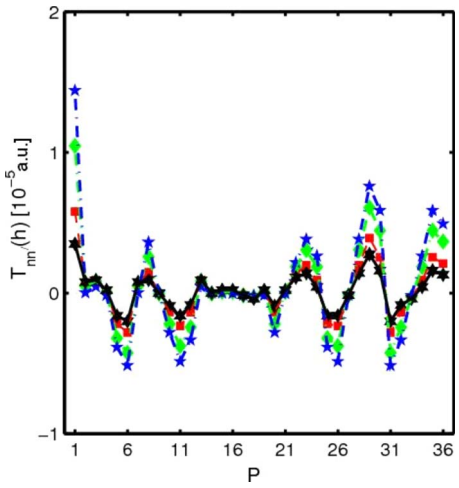

FIG. 6. (Color online) Same as in Fig. 5 but for the triplet case.

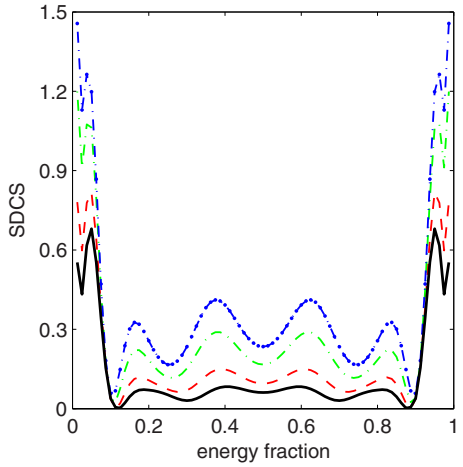

FIG. 7. (Color online) Singlet SDCS ($\pi a_0^2/Ry$) vs the energy fraction E_b/E for three different step lengths and for $T^{0*(2)}_{nn'}$ elements at 27.2 eV impact electron energy. Continuous curve, $T^{0*(2)}_{nn'}$ elements; dashed curve, for $h=0.0075$ a.u.; dash-dotted curve, for $h=0.009$ a.u.; dash-double dotted curve, for $h=0.01$ a.u. .

eV energy, in Fig. 2 for 40.8 eV energy, and in Fig. 3 for 54.4 eV energy. In Figs. 4–6 we have presented the values of $T^{1}_{nn'}$ (one indicates triplet) for three different step lengths and $T^{1*(2)}_{nn'}$ for energies of 27.2, 40.8, and 54.4 eV, respectively. Figures show that the magnitudes of $T^{s}_{nn'}$ are diminished with the decreasing of the step length. As shown in the figures, the magnitudes of $T^{s*(2)}_{nn'}$ are lowest than the values of $T^{s}_{nn'}$ for various step length. The curves were drowned joining the points square for $h=0.0075$, diamond for $h=0.009$, pentagon for $h=0.01$, and hexagon for $T^{s*(2)}_{nn'}$; show that in the figures, comparatively similar. In our previous calculation primarily to calculate the double differential cross section (DDCS), SDCS results, and triple differential cross section (TDCS)

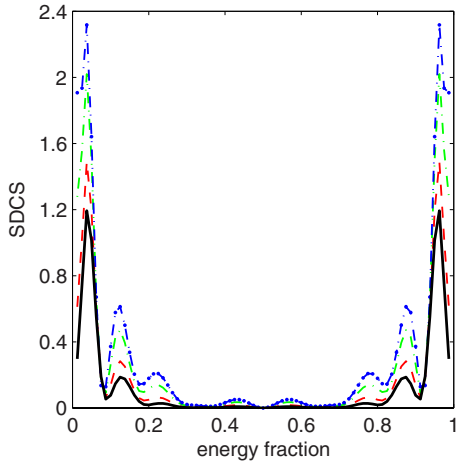

FIG. 8. (Color online) Triplet SDCS ($\pi a_0^2/Ry$) vs the energy fraction E_b/E for three different step lengths and for $T^{1*(2)}_{nn'}$ elements at 27.2 eV impact electron energy. Continuous curve, $T^{1*(2)}_{nn'}$ elements; dashed curve, for $h=0.0075$ a.u.; dash-dotted curve, for $h=0.009$ a.u.; dash-double dotted curve, for $h=0.01$ a.u. .

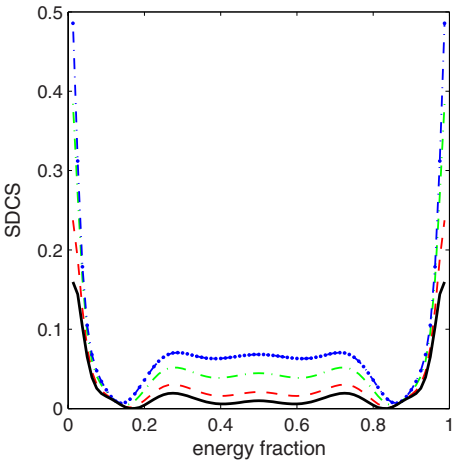

FIG. 9. (Color online) Same as Fig. 7 for 40.8 eV.

results, we established good qualitative results. There were significant discrepancies in the magnitude for extreme asymmetric energies. These types of phenomena, that happen due to the behavior of the $T^{s}_{nn'}$ elements, depend tremendously on h. At that time, we drew full electron-hydrogen problem, and it was difficult to envisage the convergence analysis with respect to step length. These figures also show that the calculation of $T^{s}_{nn'}$ elements is stable concerning h. The two-term error corrected elements $T^{s*(2)}_{nn'}$ are almost less than $T^{s}_{nn'}(0.0075)$ and in few cases equal with $T^{s}_{nn'}(0.0075)$. This implies that the two-term error correction procedure will be fruitful. In this section, we will show that the SDCS results for $T^{s*(2)}_{nn'}$ elements are significantly better than the SDCS results for $h=0.0075$ and other values. In Figs. 7–12, we have compared our calculated SDCS results for three different step lengths and for $T^{s*(2)}_{nn'}$ ($s=0$ for singlet and $s=1$ for triplet) elements. As shown in the figures, the SDCS curves are less corrugated and smaller in magnitude with a decreasing step length. The calculated SDCS results for the $T^{s*(2)}_{nn'}$ elements are smallest in magnitude and least undulating in comparison with the SDCS values for three different step lengths. In the case of singlet for 27.2 and 54.4 eV energies,

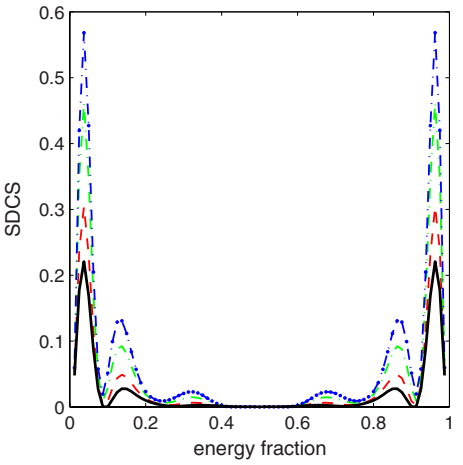

FIG. 10. (Color online) Same as Fig. 8 for 40.8 eV.

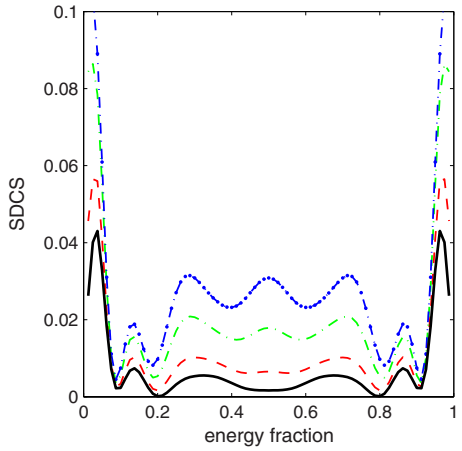

FIG. 11. (Color online) Same as Fig. 7 for 54.4 eV.

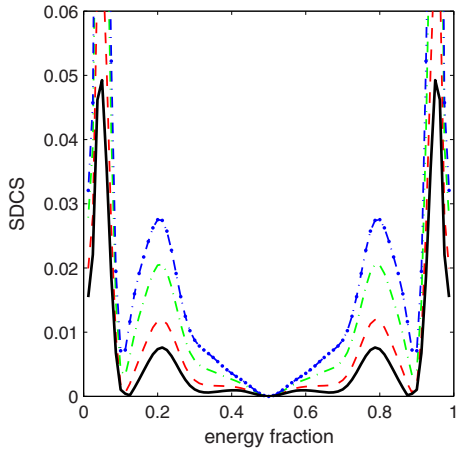

FIG. 12. (Color online) Same as Fig. 8 for 54.4 eV.

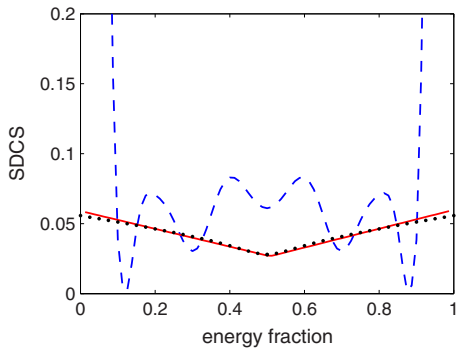

FIG. 13. (Color online) Singlet SDCS ($\pi a_0^2/Ry$) vs the energy fraction E_b/E for incident energy 27.2 eV. Continuous curve, fitted function; dashed curve, present results corresponding $T_{nn'}^{0*(2)}$ elements; dotted curve, calculated results of Jones *et al.* [10].

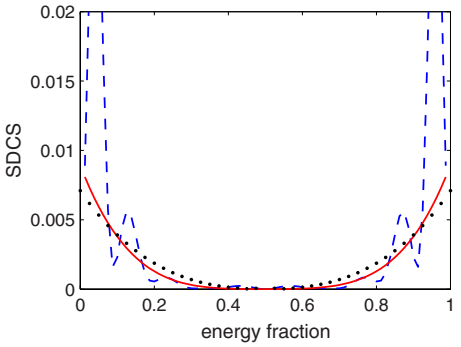

FIG. 14. (Color online) Triplet SDCS ($\pi a_0^2/Ry$) vs the energy fraction E_b/E for incident energy 27.2 eV. Continuous curve, fitted function; dashed curve, present results corresponding $T_{nn'}^{1*(2)}$ elements; dotted curve, calculated results of Jones *et al.* [10].

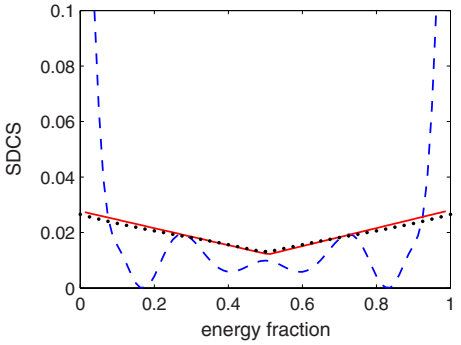

FIG. 15. (Color online) Same as Fig. 13 for 40.8 eV.

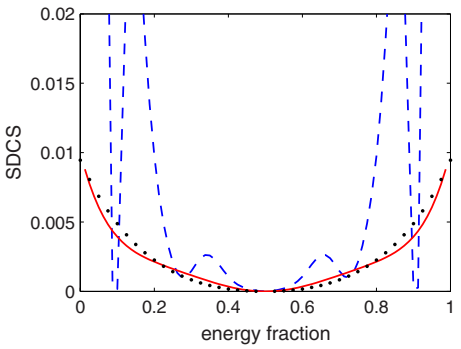

FIG. 16. (Color online) Same as Fig. 14 for 40.8 eV.

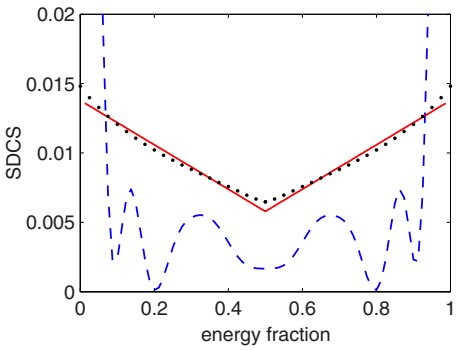

FIG. 17. (Color online) Same as Fig. 13 for 54.4 eV.

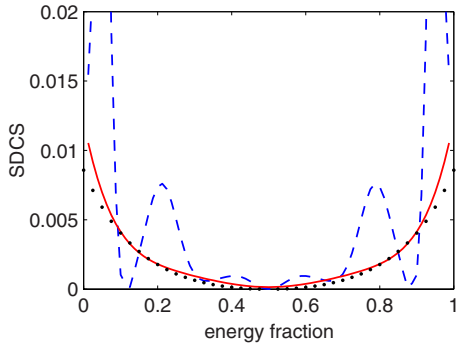

FIG. 18. (Color online) Same as Fig. 14 for 54.4 eV.

the SDCS results for $T_{nn'}^{0*(2)}$ elements are significantly different to that of for three different values of h. At 54.4 eV energy, there is an irrelevant peak at equal energy sharing case for $h=0.009$ and 0.01. The peak vanishes for $h=0.0075$ and is deep for $T_{nn'}^{0*(2)}$ elements. For 40.8 eV energy, the shape of the curves is approximately the same with the exception of magnitude. The same thing happened in the cases of the triplet, the scale of curves reduced and the wavy nature vanished. With the change of step lengths, the nature of curves change rapidly, its magnitude reduced and its wavy nature abolished swiftly with the modification of the step length, in decreasing order. The magnitude of the curves reduced significantly at the extreme asymptotic region.

VI. COMPARISON WITH BENCHMARK RESULTS

In this section, we present two-term error corrected results and fitted curves corresponding these values along with the benchmark results of Jones (see Figs. 13–18). The oscillating nature of two-term error corrected curves suggest a fit, with a proper function and a symmetry around $E/2$ (E is the energy in the final channel). We looked at the linear-linear function for singlet SDCS values ($y=a+bx+c|x-d|$ where x is the energy of the secondary electron and y is the corresponding singlet SDCS value) and a maximum six degree polynomial for the triplet SDCS data ($y=a+bx+cx^2+dx^3+ex^4+fx^5+gx^6$, where x is the energy of the secondary electron and y is the corresponding triplet SDCS value). For 27.2 eV energy, a four degree polynomial proved sufficient for curve fitting. First, we neglected broader data (maximum of eight data out of eighty) from the extreme asymptotic region, irrelevant with other data, fitted a function for the rest of the values and drew the fitted curve for the entire energy domain. In Tables I and II, we have presented the coefficients of the fitted curves for three different energies and triplet, singlet cases. Our fitted curves agree very well with the results of Jones. Sometimes, our calculated two-term error corrected results cut and touch the curves of benchmark data. It is very important for the HPW approach that our two-term error corrected results are free from any kind of scale, except triplet SDCS results at 27.2 eV which have been scaled by a factor of 0.03. In earlier DDCS and SDCS calculations, we multiplied our data by a suitable factor to lower the magnitude and compared with experimental values.

TABLE II. Coefficients for fitted curve at various impact energies and singlet case.

Energy	a	b	c	d
27.2eV	0.0405	0.00567	0.20568	0.25395
40.8eV	0.018326	0.001411	0.049555	0.864263
54.4eV	0.00373	−0.000005	0.00694	0.74947

VII. CONCLUSION

In the HPW approach, we calculate the radial part of the final state wave function numerically, which is very crucial. For evaluate appropriate cross-section results, it is essential to compute the radial part of final wave function very precisely. The condition of convergence depends on several parameters for the full electron-hydrogen problem. The model calculation is a simplification of the exact problem. Only a few parameters are involved here. In this paper we tested the dependence of the calculation of radial wave function on the step length. In the figures, presented in the paper, we have seen that with the reduction of step length, calculated SDCS results were better (smooth and less magnitude). By using the values of $T_{nn'}^{s}$, elements for three different step lengths, we have been able to calculate two-term error corrected SDCS results. Comparison of the two-term error corrected SDCS results with that of for three different step lengths shows that our endeavor to calculate error corrected results has been fruitful. Our computed error corrected results are less satisfactory, still there are some oscillations. Although the magnitude of our evaluated results is quite relevant except when in the extreme asymptotic energy region. The main difficulty is that when we diminish the step length, the number of mesh points is increased so there is a limitation of digital manipulation. The fitted curves corresponding

TABLE I. Coefficients for the fitted curve at various impact energies and triplet case.

Energy	a	b	c	d	e	f	g
27.2eV	0.042012	−0.650385	3.8148108	−10.0556766	10.054884		
40.8eV	0.046054	−0.49753	2.90446	−9.505798	16.482738	−14.075808	4.691936
54.4eV	0.0563445	−0.420831	1.529658	−3.071799	3.3675705	−1.874718	0.416538

equipped error corrected SDCS data agree excellently with the benchmark results of Jones *et al.* [10]. If one considers a higher point finite difference scheme with the error term is of the order of h^{12}. At this point, it is possible to avoid the use of the two-term error correction. However, it will be more difficult to compute a higher finite difference scheme. From this point of view, two-term error correction is particularly significant.

[1] J. N. Das, S. Paul, and K. Chakrabarti, Phys. Rev. A **67**, 042717 (2003).
[2] J. N. Das, K. Chakrabarti, and S. Paul, J. Phys. B **36**, 2707 (2003).
[3] J. N. Das, K. Chakrabarti, and S. Paul, Phys. Lett. A **316**, 400 (2003).
[4] J. N. Das, K. Chakrabarti, and S. Paul, Phys. Rev. A **69**, 044702 (2004).
[5] J. N. Das, S. Paul, and K. Chakrabarti, Phys. Rev. A **72**, 022725 (2005).
[6] J. N. Das, S. Paul, and K. Chakrabarti, Eur. Phys. J. D **39**, 223 (2006).
[7] A. Temkin, Phys. Rev. **126**, 130 (1962).
[8] R. Poet, J. Phys. B **11**, 3081 (1978).
[9] S. Jones and A. T. Stelbovics, Phys. Rev. Lett. **84**, 1878 (2000).
[10] S. Jones and A. T. Stelbovics, Phys. Rev. A **66**, 032717 (2002).
[11] R. Poet, J. Phys. B **13**, 2995 (1980).
[12] I. Bray, Phys. Rev. Lett. **78**, 4721 (1997).
[13] C. W. McCurdy, D. A. Horner, and T. N. Rescigno, Phys. Rev. A **63**, 022711 (2001).
[14] N. Miyashita, D. Kato, and S. Watanabe, Phys. Rev. A **59**, 4385 (1999).
[15] J. N. Das, S. Paul, and K. Chakrabarti, AIP Conf. Proc. **697**, 82 (2003).
[16] T. W. Shyn, Phys. Rev. A **45**, 2951 (1992).
[17] R. G. Newton, *Scattering Theory of Waves and Particles* (McGraw-Hill, New York, 1966).
[18] S. Paul (private communication).